BMC Plant Biology

RESEARCH

Open Access

Elucidating the mechanism of resistance to anthracnose in litchi leaves through transcriptome analysis

Fang Li[1†], Ji Wu[1,2†], Lei Zhang[3], Qiying Lin[1], Xueren Cao[1], Huanling Li[1], Shujun Wang[1], Guo Wang[1], Xiaoxu Li[1] and Jiabao Wang[1*]

Abstract

Background Litchi, an important tropical fruit, is severely affected by anthracnose disease. However, the mechanism of its disease resistance response remains unknown, and resistant accession genetic resources and resistance-related genes have not yet been identified.

Results In this study, 82 accessions of litchi were evaluated for resistance to *Colletotrichum gloeosporioides*, and the accessions 'Haiken 5' and 'Nongmei 5 hao' were identified as resistant and susceptible, respectively. Leaves from these two accessions were inoculated with *C. gloeosporioides* and collected at 6 and 24 h for use as materials for transcriptome analysis. Analyses of the differentially expressed genes (DEGs) between the accessions and their controls, which were inoculated with potato dextrose agar medium, revealed that the resistant accession presented more DEGs with smaller changes in magnitude, whereas the susceptible accession presented fewer DEGs with greater changes in magnitude. Gene Ontology (GO) and Kyoto Encyclopedia of Genes and Genomes (KEGG) pathway analyses were performed, and phenylpropanoid biosynthesis, amino sugar and nucleotide sugar metabolism, and plant–pathogen interactions were identified as common pathways. Chitinase activity, oxidoreductase activity, aminoglycan and glucosamine-containing compounds, and cell wall metabolic processes also participated in the defence reaction. Salicylic acid signalling in litchi leaves contributed to resistance to *C. gloeosporioides*. Short Time-series Expression Miner (STEM) and weighted correlation network analysis (WGCNA) were also employed to evaluate the gene expression trends and identify highly correlated genes.

Conclusion Litchi accessions presented different resistance responses to anthracnose disease. Small changes in the expression levels of critical resistance-related genes were sufficient to produce the defence reaction. Calcium ion regulatory mechanisms and transcription factors have been preliminarily identified as contributors to disease resistance. Multiple pathways and molecular processes participate in the defence response. These results identify candidate genes and pathways involved in litchi plant defence against anthracnose.

Keywords *Litchi chinensis* Sonn., Anthracnose disease, Resistance response, Differentially expessed genes

†Fang Li and Ji Wu contributed equally to this work.

*Correspondence:
Jiabao Wang
wangjiabao@catas.cn
[1]Environment and Plant Protection Institute, Danzhou Scientific Observing and Experimental Station of Agro-Environment, Chinese Academy of Tropical Agricultural Sciences, Haikou, Hainan province 571101, China
[2]National Key Laboratory for Cultivar Innovation and Utilization for Fruit and Vegetable Horticultural Crops, Huazhong Agricultural University, Hubei province 430070 Wuhan, China
[3]Tropical Crops Genetic Resources Institute, Chinese Academy of Tropical Agricultural Sciences, Haikou, Hainan province 571101, China

Introduction

Colletotrichum causes typical anthracnose symptoms, such as black spots on leaves and sunken necrotic lesions on fruit. This fungus affects a wide range of host plants worldwide, and it is one of the most destructive diseases in commercial fruit production [1–4]. Litchi (*Litchi chinensis* Sonn.) is an important tropical fruit that originated in southern China and is known as 'the queen of fruit' [5]. *Colletotrichum* species are among the most serious pathogens of litchi; the symptoms caused by these fungi occur throughout the whole growth cycle [6–8]. The most severe damage is caused by *C. gloeosporioides* [7], which attacks leaves, stems, and fresh and postharvest fruit, resulting in a decrease in photosynthesis and fruit pericarp browning and rot [8]. *C. gloeosporioides* colonize the pericarp surface at the young litchi fruit stage. The pathogen proliferates following fruit development, at which stage the fruits are asymptomatic. Outbreaks can occur during storage and transportation in a humid environment.

As *C. gloeosporioides* can be eliminated by fungicide application to litchi, physical sterilization, biological control [10], and cultural techniques are often not taken seriously. Fungicide application is not expensive but it affects the environment and ecosystem health. Wang et al. reported that 100% of litchi fruits contained at least 1 pesticide residue [9]. Resistant phenotype screening and mechanistic research are effective strategies for breeding resistant accessions.

Plants have evolved a multilayered immune system to resist pathogens. The cell wall is an important barrier to pathogen invasion and is reinforced by pathogen stimulation. Pattern-triggered immunity (PTI) is the primary type of immunity in plants. Pattern-recognition receptors (PRRs) recognize pathogen-associated molecular patterns (PAMPs) to induce mitogen-activated protein kinases, calcium signals, transcription factors (TFs), hormone signals, and other types of defence signalling. The second type of plant immunity is effector–trigger immunity (ETI). Nucleotide-binding leucine-rich repeat proteins can be specifically activated by effectors, triggering immunity to inhibit pathogen infection and growth. These two types of immune signalling are synergistic; PTI is promoted by ETI via PTI signalling, and mitogen-activated protein kinases (MAPKs) and NADPH oxidase can effectively ensure ETI [11].

Screening to identify resistant accessions and analysing resistance mechanisms are reliable methods for controlling pathogen invasion. High-throughput RNA sequencing (RNA-seq) is an important approach because it provides a comprehensive transcriptome profile in plants to elucidate plant infection and defence mechanisms [12, 13]. Genes associated with resistance can be identified by comparing the transcriptomes of resistant and susceptible accessions after infection with pathogens and can serve as critical genetic resources in resistance breeding. However, few studies have investigated resistance mechanisms and genes related to the regulation of litchi–pathogen interactions.

In this study, litchi accession resources were evaluated for resistance to *C. gloeosporioides*, and resistant and susceptible accessions were studied further via high-throughput RNA-seq to explore the differentially expressed genes (DEGs) induced in response to pathogen infection. Genes and metabolic pathways with important functions in the response to *C. gloeosporioides* infection were identified. These results provide a foundation for better understanding the molecular defence response of litchi and enabling resistance breeding.

Results

Evaluation of litchi accession resources for *C. gloeosporioides* resistance

Eighty-two litchi accessions were screened for resistance to *C. gloeosporioides* in three tests, which were performed in September 2021, March 2022 and July 2022 (Supplementary Materials Table S1). Brown disease spots were observed, and the spot area was measured at 72 h postinoculation (hpi). The spot areas of the 82 accessions presented a continuous distribution, but the incidence rates and spot areas of the resources were not consistent across the three replications (Fig. 1a), with averages of 20.84, 21.10, and 37.58 mm^2. One resource, 'Cangdao 5', exhibited immunity to *C. gloeosporioides* at the first evaluation timepoint after inoculation, and three resources, 'Cuirou', 'A13', and 'Haiken 18', exhibited immunity to *C. gloeosporioides* at the second evaluation timepoint. However, no resources showed immunity to *C. gloeosporioides* at the third evaluation timepoint. For resources, 'Haiken 5', 'Haiken 2 hao', and 'Zili', presented high disease resistance with smaller lesion areas, and 'Nongmei 5 hao', 'Ruhong 7', and '13Y04' presented low disease resistance with larger lesion areas and severe symptoms.

Compared with the 'Nongmei 5 hao' accession, the 'Haiken 5' accession was more tolerant to *C. gloeosporioides*. Therefore, these accessions were selected as the materials for further analysis. To confirm the results of the screen, the incidence and spot areas of these accessions were measured in more detail. Anthracnose lesions were observed at 24 hpi (Fig. 1b, c), and typical disease spots were observed on the susceptible (S) accession but not on the resistant (R) accession. The anthracnose lesion areas increased with time after inoculation. A significant difference in spot area between the accessions was observed beginning at 24 hpi (Fig. 1c).

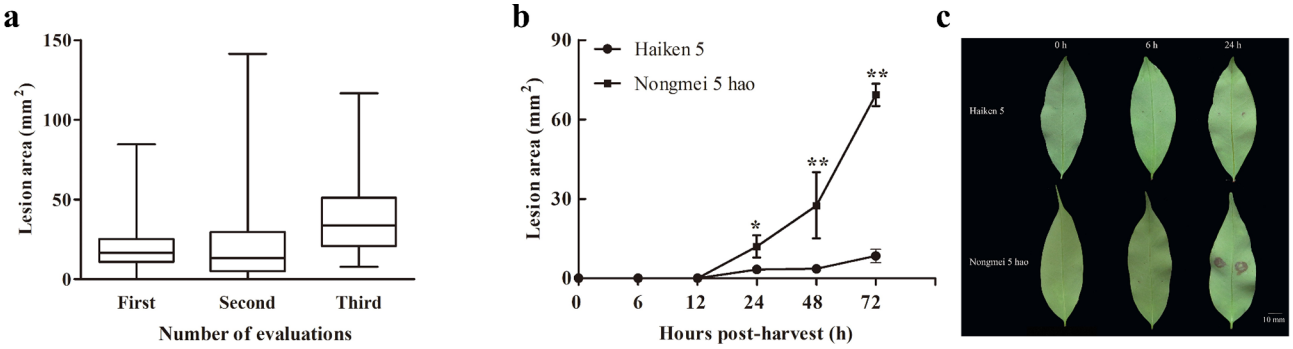

Fig. 1 Disease area and phenotype of litchi leaves inoculated with *Colletotrichum gloeosporioides*. (**a**) Disease area of 82 litchi accessions at 72 h after inoculation with *C. gloeosporioides*. (**b**) Changes in disease area in 'Haiken 5' and 'Nongmei 5 hao' leaves from 0-72 h after inoculation. The data are expressed as the means ± standard deviations. Asterisks indicate that values are significantly different between 'Haiken 5' and 'Nongmei 5 hao' according to Student's *t* test (* $P<0.05$, ** $P < 0.01$). (**c**) Phenotypes of 'Haiken 5' and 'Nongmei 5 hao' leaves at 0, 6, and 24 h after inoculation. Scale bar = 10 mm

Analysis of differential gene expression in response to anthracnose infection via transcriptome sequencing

For DEG identification, transcriptome sequencing of the two accessions was performed, with 'Haiken 5' as the R accession and 'Nongmei 5 hao' as the S accession. Both accessions were inoculated with *C. gloeosporioides*, and the leaves were sampled for transcriptome sequencing. On the basis of the phenotypic analyses, 0, 6, and 24 hpi were selected as the leaf collection timepoints because they represented no infection, early-stage infection and late-stage infection, respectively. The leaves were mock inoculated with ddH_2O as the control. In total, 13,119,300 raw data reads were generated from 30 samples, and 12,824,400 clean data reads were obtained. Together, the samples generated a total of 192.39 Gb of clean data. The average Q20 (reads with a mean error rate < 1%) and Q30 (reads with a mean error rate < 0.1%) values were 96.23 and 90.46%, respectively. Clean reads from the samples were mapped to the litchi genome (http://www.sapindaceae.com/). The mapping rate ranged from 80.64 to 85.48% (Table S2). Principal component analysis (PCA) was also performed for each accession and treatment (Fig. S2).

Upregulated and downregulated DEGs were identified through transcriptome analysis of both the infected and mock-inoculated samples. To characterize the resistance mechanisms involved in the response to *C. gloeosporioides*, we first identified the DEGs between anthracnose-infected leaves and mock-inoculated leaves at 6 and 24 hpi. The transcriptional responses of the R and S accessions to *C. gloeosporioides* were distinct. Compared with the uninfected leaves, including the noninoculated leaves (at 0 h) and mock-inoculated leaves at 6 and 24 hpi, the R accession exhibited 400 and 571 DEGs, respectively, and the S accession exhibited 363 and 439 DEGs at 6 and 24 hpi, respectively. A Venn diagram was constructed to show the overlapping DEGs between the R and S accessions (Fig. 2a and b). Overall, 135 and 177 DEGs in the two accessions were involved in the response to *C. gloeosporioides* at 6 and 24 hpi, respectively (Fig. 1a and b). An analysis of 135 common DEGs at 6 hpi revealed 99 upregulated DEGs and 36 downregulated DEGs in the R and S accessions, respectively, compared with the mock-inoculated control (Fig. 2c and e). Among the 177 common DEGs at 24 hpi, 164 were upregulated and 13 were downregulated in the R accession in response to *C. gloeosporioides*. In the S accession, 163 DEGs were upregulated, and 14 were downregulated (Fig. 2d and f). The expression of EP1-like glycoprotein 2 (LITCHI012883.m1) was consistently upregulated in the R accession but not in the S accession. A total of 265 and 394 DEGs were identified in the R accession, and 228 and 262 DEGs were identified in the S accession at 6 and 24 hpi, respectively. The DEGs in the R accession were primarily hormone signalling-related genes and cytochrome P450s and enzymes, such as serine/threonine-protein kinases, laccases, and transferases.

Compared with the S accession, the R accession presented more DEGs at 6 and 24 hpi. DEGs between the infected and mock-inoculated samples were clearly illustrated via heatmap cluster analysis; two and three clusters were detected at 6 and 24 hpi, respectively (Fig. 2e, f). The number of downregulated genes was greater than that of upregulated genes.

Functional enrichment evaluation was performed for the DEGs via Gene Ontology (GO) and Kyoto Encyclopedia of Genes and Genomes (KEGG) pathway annotation. For the 400 DEGs in the R accession at 6 hpi, 328 GO terms were identified, of which 38, comprising 8 molecular function (MF) terms and 30 biological process (BP) terms, were identified as significantly enriched (Fig. 3a, Table S3). A total of 332 GO pathways were specifically enriched among the 571 DEGs in the R accession, and 43 GO terms were significantly enriched, including 1 cellular component (CC), 28 MF, and 14 BP terms, at 24 hpi (Fig. 3b, Table S4). Among the 242 enriched GO pathways, 34 pathways, including 7 MF and 27 BP terms and

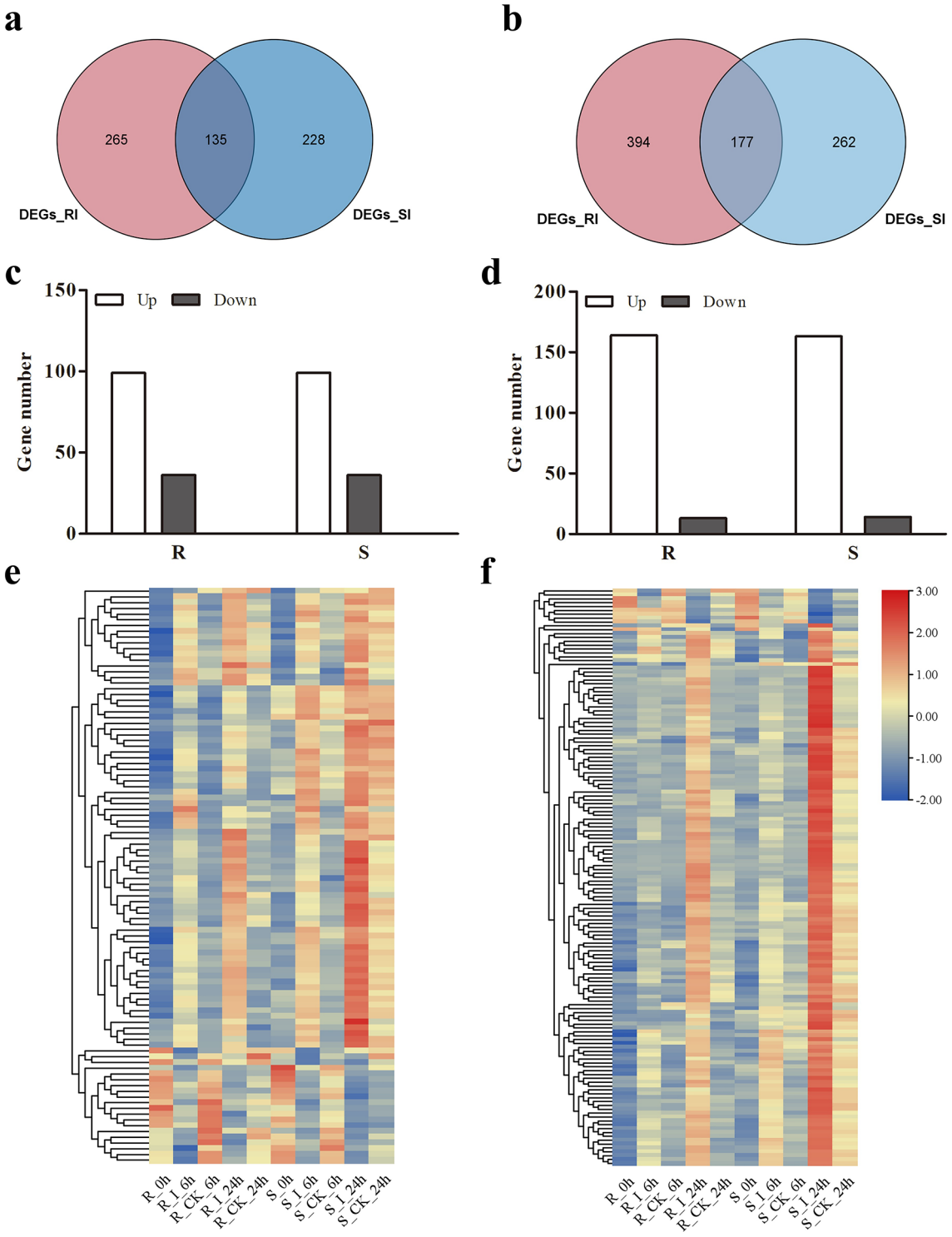

Fig. 2 Analysis of differentially expressed genes (DEGs) in litchi leaves in response to *Colletotrichum gloeosporioides* inoculation at 6 and 24 h postinoculation (hpi). (**a**, **b**) Venn diagrams of DEGs in 'Haiken 5' (R) and 'Nongmei 5 hao' (S) at 6 and 24 hpi, respectively; (**c**, **d**) Analysis of upregulated and downregulated DEGs after infection with *C. gloeosporioides* at 6 and 24 hpi for the R and S accessions, respectively. (**e**) Heatmap analysis of 135 DEGs common to the R and S accessions at 6 hpi (partial). (**f**) Heatmap analysis of 177 DEGs common to the R and S accessions at 24 hpi (partial)

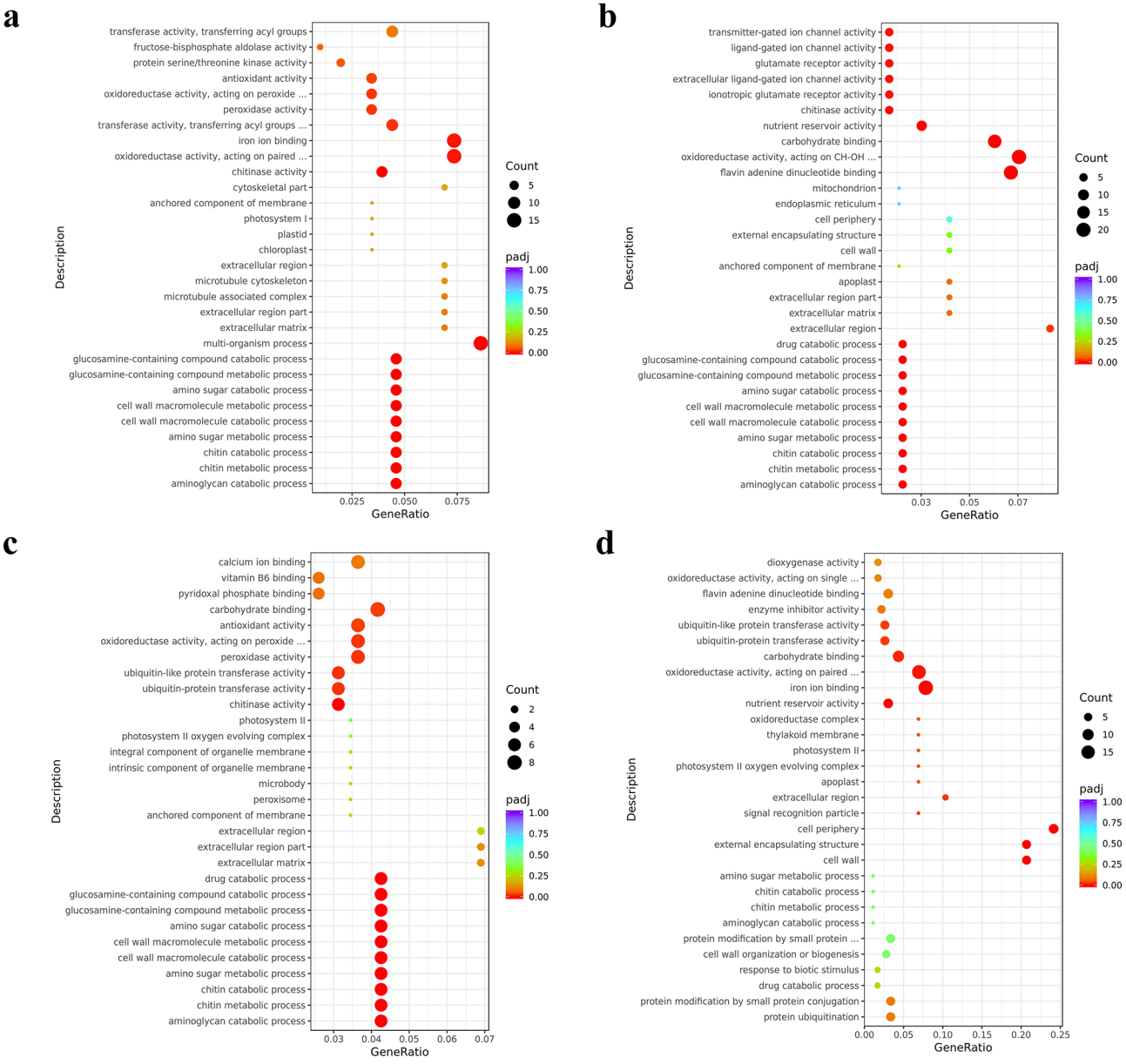

Fig. 3 Gene Ontology (GO) enrichment of differentially expressed genes (DEGs) in 'Haiken5' (R) and 'Nongmei 5 hao' (S) in response to *Colletotrichum gloeosporioides* inoculation. (**a**, **b**) GO enrichment of the R accession DEGs at 6 (**a**) and 24 hpi (**b**). (**c**, **d**) GO enrichment of the S accession DEGs at 6 (**c**) and 24 hpi (**d**)

comprising 363 DEGs, were significantly enriched in the S accession at 6 hpi (Fig. 3c, Table S5). Among the 439 DEGs in the S accession, 382 GO pathways were identified in both accessions at 24 hpi, of which 16 pathways, including 10 CC and 6 MF terms, were significantly enriched (Fig. 3d, Table S6). No CC terms were significantly enriched at 6 hpi in either the R or S accession. More GO terms were enriched in the R accession than in the S accession at 6 hpi, and many GO terms, such as peroxidase activity, aminoglycan catabolic and metabolic process, and cell wall macromolecule catabolic and metabolic process, were enriched among the DEGs in the R accession at 6 and 24 hpi. There were 26 common GO terms significantly enriched between the R and S accessions at 6 hpi; the R accession had 12 unique GO terms, and the S accession had 8. At 24 hpi, there were 39 GO terms unique to the S accession, 12 GO terms unique to the S accession, and 4 GO terms common to both accessions.

From the 400 DEGs in the R accession, 54 KEGG pathways were identified at 6 hpi, with 6 pathways identified as significantly enriched (Fig. 4a, Table S7). In the R accession, 60 KEGG pathways were enriched among the 571 DEGs at 24 hpi, including 5 significantly enriched

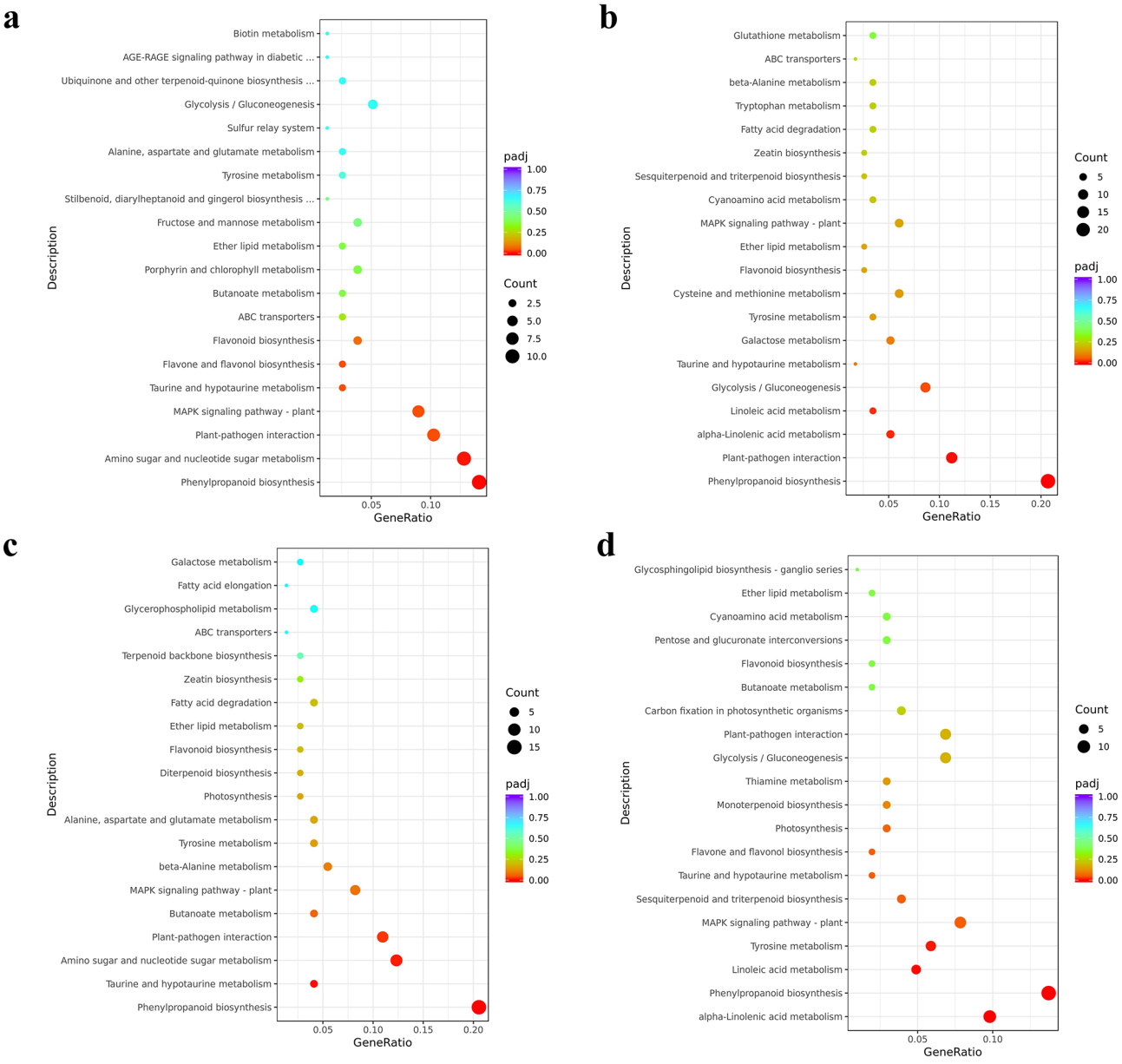

Fig. 4 Kyoto Encyclopedia of Genes and Genomes (KEGG) pathway enrichment of differentially expressed genes (DEGs) from 'Haiken 5' (R) and 'Nongmei 5 hao' (S) in response to *Colletotrichum gloeosporioides* inoculation. (**a**, **b**) KEGG enrichment of the R accession DEGs at 6 (**a**) and 24 hpi (**b**). (**c**, **d**) KEGG enrichment of the S accession DEGs at 6 (**c**) and 24 hpi (**d**)

pathways (Fig. 4b, Table S8). Phenylpropanoid biosynthesis and plant–pathogen interactions were significantly enriched at both 6 and 24 hpi. For the 363 DEGs in the S accession, 42 KEGG pathways were enriched at 6 hpi, including 4 pathways that were significantly enriched (Fig. 4c, Table S9). At 24 hpi, 59 KEGG pathways were enriched among the 439 DEGs in the S accession, of which 4 pathways were significantly enriched (Fig. 4d, Table S10). Phenylpropanoid biosynthesis, amino sugar and nucleotide sugar metabolism, and plant–pathogen interactions were common significantly enriched pathways at 6 hpi. Phenylpropanoid biosynthesis, linoleic acid metabolism, and alpha-linolenic acid metabolism were significantly enriched at 24 hpi after *C. gloeosporioides* infection. More pathways were enriched in the R accession than in the S accession. Pathways such as the MAPK signalling pathway and flavone and flavonol biosynthesis were specifically significantly enriched in the R accession.

STEM analysis identified the expression profiles of DEGs in response to anthracnose infection

DEGs from R and S accessions at different evaluation timepoints were clustered according to their expression values via short time series expression miner (STEM).

The DEGs were divided into 9 profiles according to their expression trends (Fig. 5, Tables S11 and S12). The gene expression trend profiles were similar for the R and S accessions. A total of 5 significantly different clusters were obtained after inoculation of the R accession, and 6 were obtained for the S accession. The DEGs in profiles 2, 4, and 5 of the R accession and profiles 1 and 4 of the S accession gradually increased in expression over time. The number of DEGs in profiles 3 and 6 of the R accession and profiles 2 and 3 of the S accession gradually decreased. The DEGs in profile 1 of the R accession and profiles 5 and 6 of the S accession showed fluctuating trends. The upregulated DEGs in profile 4 (248) of the R accession and profile 1 (245) of the S accession represented the largest number of genes. The KEGG pathways enriched among the 5 profiles comprising upregulated DEGs were similar in the R and S accessions (Figs. S2 and S3), namely, phenylpropanoid biosynthesis, taurine and hypotaurine metabolism, amino sugar and nucleotide sugar metabolism, and plant–pathogen interactions. Phenylpropanoid biosynthesis was the only pathway enriched in all 5 profiles. The GO terms chitinase activity, oxidoreductase activity, glycosaminoglycan catabolic process, cell wall macromolecule catabolic process, drug catabolic process, and protein ubiquitination were also enriched in these profiles. The downregulated DEGs in profiles 3 and 6 of the R accession and profiles 2 and 3 of the S accession comprised the second largest clusters, but there were no commonly enriched GO terms or KEGG pathways. The term photosynthesis-related was enriched in the S accession, and the terms oxidoreductase activity and nucleotide catabolic process were enriched in the R accession. Profile 1 of the R accession and profile 6 of the S accession tended to increase but then decreased in response to *C. gloeosporioides* infection. These genes were commonly significantly enriched in the following GO terms: cell recognition, pollination, pollen–pistil interaction, multicellular organism process, recognition of pollen, reproduction, reproductive process, multiorganism process, and multicellular organismal process.

Identification of coexpressed modules and hub genes

To identify the highly correlated genes and hub genes that respond to *C. gloeosporioides* inoculation, weighted correlation network analysis (WGCNA) was performed (https://github.com/ShawnWx2019/WGCNA-shinyApp). By combining the RNA-seq and phenotypic data, 6000 genes were identified and used to construct 18 modules with consistent expression patterns (Fig. 6a). Among the 18 coexpression modules, 2 were significantly correlated with disease resistance-related traits (Fig. 6b): the greenyellow module was positively correlated with inoculation of the R accession at 24 hpi (correlation coefficient of 0.76), and the turquoise module was significantly positively correlated with inoculation of the S accession at 24 hpi (correlation coefficient of 0.90). The different gene expression modules involved in pathogenic interactions were subjected to GO and KEGG enrichment analyses (Tables S13 to S6). GO enrichment analysis revealed that the genes in the turquoise module were significantly enriched in 22 pathways, such as the aminoglycan catabolic process, chitin metabolic process, cell wall macromolecule catabolic process, glucosamine-containing compound metabolic process, and carbohydrate derivative catabolic process (Table S13). The KEGG pathways associated with amino sugar and nucleotide sugar metabolism, plant–pathogen interactions, glutathione metabolism and alpha-linolenic acid metabolism were significantly enriched in the turquoise module (Table S14). The GO terms enriched among the genes in the greenyellow module were enriched in cellular amino acid metabolic processes, cysteine metabolic processes, cysteine biosynthetic processes from serine, etc. (Table S15). The

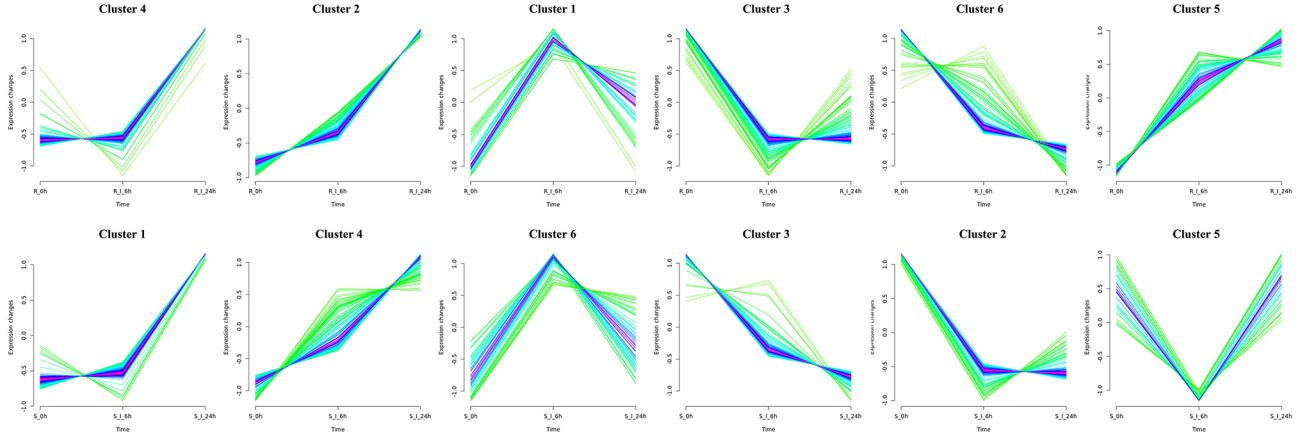

Fig. 5 Short time series expression miner (STEM) analysis of the differentially expressed genes (DEGs) from 'Haiken 5' (R) and 'Nongmei 5 hao' (S) in response to *Colletotrichum gloeosporioides* inoculation

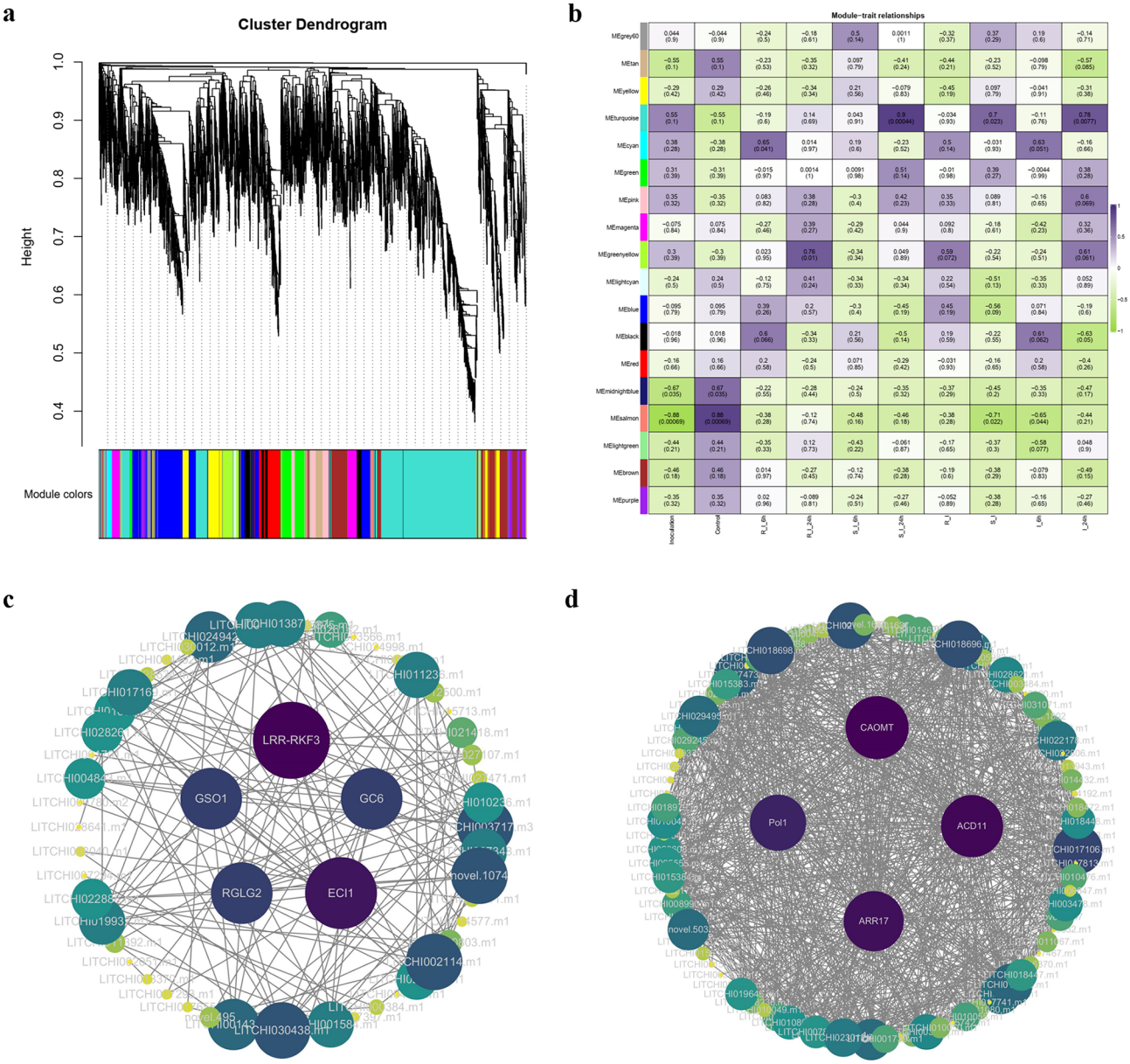

Fig. 6 Weighted gene coexpression network analysis (WGCNA) of litchi infection with *Colletotrichum gloeosporioides*. (**a**) Gene coexpression modules identified by gene expression and sample. Eighteen modules of coexpressed genes were identified; different colours indicate different modules. (**b**) Heat map of correlations between sample traits and modules. The colour of the bar represents the level of correlation. (**c**, **d**) Gene-gene interaction network analysis to identify the hub genes from the greenyellow (**c**) and turquoise (**d**) modules

enriched KEGG pathways among greenyellow modules included alanine, aspartate and glutamate metabolism; biotin metabolism; porphyrin and chlorophyll metabolism; and aminoacyl-tRNA biosynthesis (Table S16). Gene coexpression networks were constructed using Cytoscape software [14], and the hub genes with the largest number of network interactions were highlighted. The hub genes were associated primarily with enzymes. These genes, such as enoyl-CoA delta isomerase 3 (LITCHI015365.m1, ECI1), LRR receptor-like serine/threonine-protein kinase RKF3 (LITCHI003864.m1, LRR-RKF3), LRR receptor-like serine/threonine-protein kinase GSO1 (LITCHI031193.m1,GSO1), Golgin candidate 6 (LITCHI020614.m1, GC6), E3 ubiquitin-protein ligase RGLG2 (LITCHI029848.m1, RGLG2), caffeic acid 3-O-methyltransferase (LITCHI021780.m1, CAOMT), ACD11 homolog protein (LITCHI005513.m1, ACD11), Thaumatin-like protein 1 (LITCHI018696.m1, TLP), DNA-directed RNA polymerase 1, and mitochondrial (LITCHI026096.m1, Pol1), might play important roles in resistance to *C. gloeosporioides*. Moreover, the results

showed that protein ubiquitination was associated with ETI signalling.

Effects of *C. gloeosporioides* infection on transcription factor expression

TFs regulate gene expression in response to stress. The AP2/ERF, bHLH, bZIP, MYB, NAC, P450, and WRKY families are the TFs most closely related to plant immunity. In this study, 251 TF genes representing 95 families were identified from the DEGs as modulating a cascade of resistance reactions at 6 hpi. Among these genes, the AP2/ERF, MYB, bHLH, WRKY, P450, and Pkinase genes were further analysed, and their expression levels were significantly induced or inhibited (Fig. 7). In the R accession, 27 TFs were upregulated, and 26 were downregulated. In contrast, in the S accession, 24 TFs were upregulated, and 28 were downregulated. Most of the TF genes presented greater degrees of change in expression in response to *C. gloeosporioides* inoculation in the S accession than in the R accession.

Validation of RNA-Seq data by RT–qPCR analysis

To confirm the relative gene expression observed in the RNA-seq data, RT–qPCR was performed for eight DEGs. Eight genes were selected based on comprehensive evaluation of expression levels and involvement in metabolic pathways following *C. gloeosporioides* infection in both R and S accessions (Fig. 8, Table S17). These genes included calcium uptake protein, mitochondrial (LITCHI019758.m1, *MCU*); patatin-like protein 2 (LITCHI011067.m1, *PLP2*); WRKY transcription factor 72 (LITCHI005126.m1, *WRKY 72*); calcium-binding allergen Bet v 3 (LITCHI019645.m1, *CML42*); plant cysteine oxidase 1 (LITCHI003402.m1, *PCO1*); aldehyde dehydrogenase family 2 member B4, mitochondrial (LITCHI004973.m1, *ALDH2*); ABC transporter G family member 24

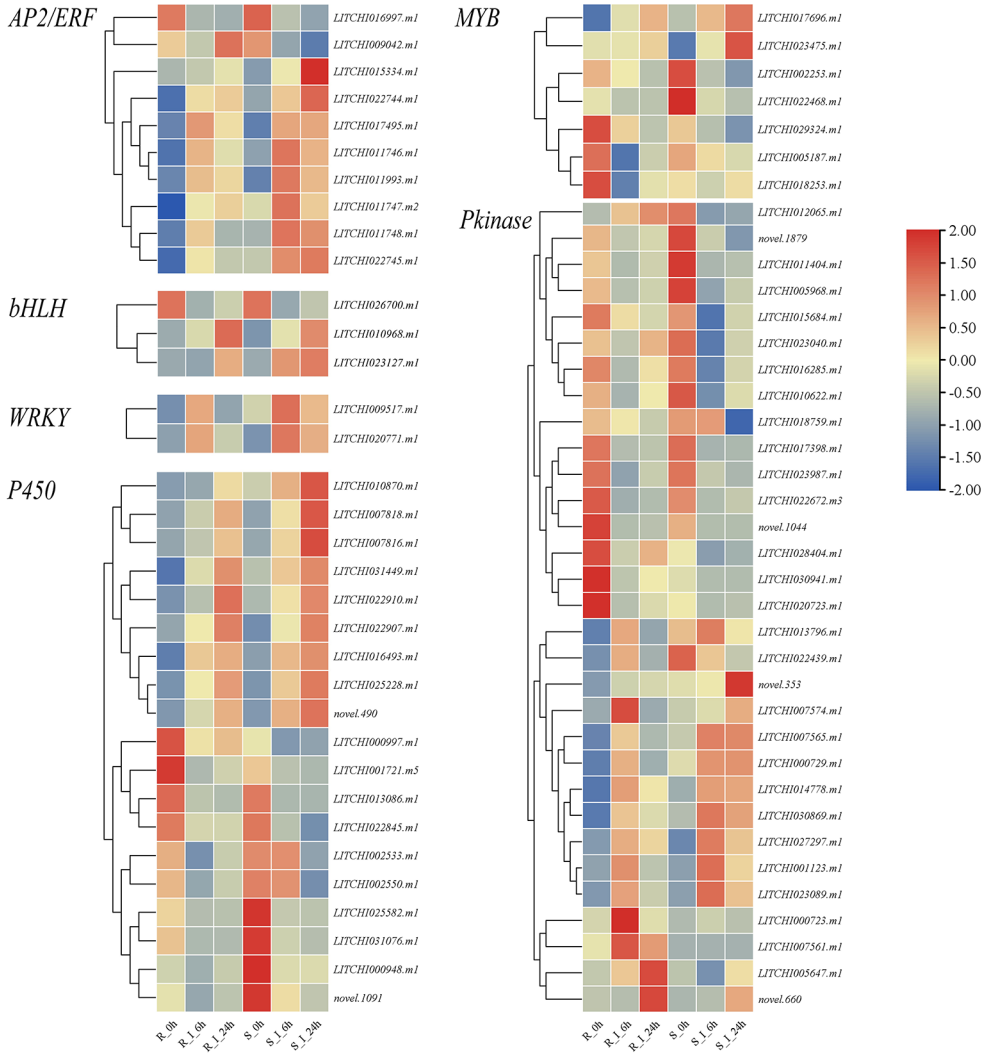

Fig. 7 Heatmap of transcription factor (TF) expression in 'Haiken 5' (R) and 'Nongmei 5 hao' (S) in response to *Colletotrichum gloeosporioides* infection. The expression levels are represented by the colour bar. I: inoculated with *C. gloeosporioides*

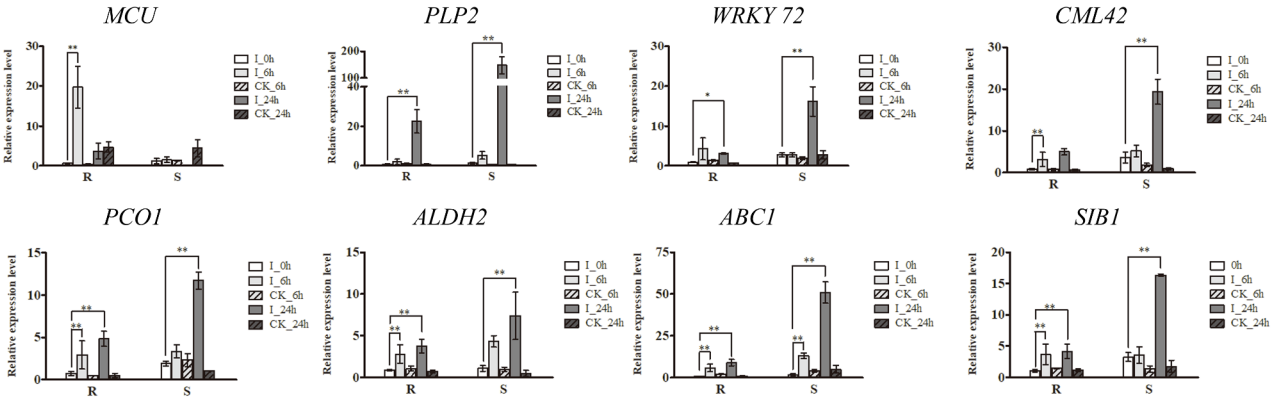

Fig. 8 Gene expression level validation by qRT–PCR analysis in 'Haiken 5' (R) and 'Nongmei 5 hao' (S) after *Colletotrichum gloeosporioides* infection. Asterisks indicate that values are significantly different between plants inoculated with *C. gloeosporioides* and the control via Student's t test (* $P \leq 0.05$, ** $P \leq 0.01$).

Fig. 8 Gene expression level validation by qRT-PCR analysis in 'Haiken 5' (R) and 'Nongmei 5 hao' (S) after *Colletotrichum gloeosporioides* infection. Asterisks indicate that values are significantly different between plants inoculated with *C. gloeosporioides* and the control via Student's t test (* $P<0.05$, ** $P<0.01$)

(LITCHI027843.m1, *ABC1*); and sigma factor binding protein 1 (LITCHI019832.m1, *SIB1*). The relative gene expression in the R and S accessions was consistent with the expression patterns in the RNA-seq data, validating its accuracy. The *MCU* gene exhibited differential expression only at 6 hpi in the R accession. The other seven genes were differentially expressed in both accessions following inoculation with *C. gloeosporioides*, with greater expression changes observed in the S accession than in the R accession.

Discussion

Anthracnose is one of the most destructive agricultural diseases, occurring in nearly all crops. Accession screening and defence mechanism analysis are the major strategies for resistance breeding and loss reduction [15, 16]. Litchi is affected by multiple diseases; however, its response mechanisms have not been reported, and the breeding of resistant accessions has been limited. In this study, we assessed the resistance of accessions in response to *C. gloeosporioides* inoculation and identified representative R and S accessions. Through further analyses of these accessions, resistance genes, response modules, and pathways were revealed.

Disease resistance capacity is affected by various factors, including tree and leaf age, the temperature and humidity of the environment, fertility, illumination, antibiotic application, and cultivation management [17–22]. In this study, three evaluations were performed to test disease resistance under different seasonal climate patterns. In Hainan, the temperature in September and July is higher than that in March, and litchi is in a period of rapid growth; thus, the average lesion areas were larger at these times. Resistance evaluations were performed with mycelial agar disks because litchi leaf postures vary such that *C. gloeosporioides* spore suspensions will flow off the surfaces of most leaf blades, even with the addition of a surfactant.

Gene expression levels were determined via transcriptome analysis, and DEGs were identified on the basis of their expression at different times after inoculation. Compared with the S accession, the R accession presented more DEGs that participated in the response to *C. gloeosporioides* inoculation, and their involvement in the disease response increased over time (Fig. 2a and b). However, the changes in the magnitude of gene expression were much smaller in the R accession than in the S accession (Fig. 2e and f). This phenomenon has also been observed in tea [23]. The DEGs of the R accession presented more enriched pathways than those of the S accession did (Figs. 3 and 4). These findings revealed that more DEGs and pathways were activated in response to pathogen infection in the R accession than in the S accession and that greater changes in gene expression were not effective in controlling *C. gloeosporioides* infection in the S accession.

The KEGG pathways enriched in response to pathogens nearly always include phenylpropanoid biosynthesis [23–25], plant–pathogen interaction [26], the flavonoid biosynthesis pathway [27], and plant hormone signals [28]. In this study, the KEGG pathways enriched among the DEGs were different for the R and S accessions. Pathways associated with disease resistance were enriched, and amino sugar and nucleotide sugar metabolism and glycolysis/gluconeogenesis pathways were significantly enriched, indicating that a glucometabolic response is also involved in litchi resistance to the pathogen. The amino sugar and nucleotide sugar metabolism pathway is related to stress [29] and is relevant to cell wall synthesis and repair in the resistance response [30]. Multiple

sucrose metabolism pathways, including fructose and mannose metabolism and glucosinolate biosynthesis, also participate in the response to *C. gloeosporioides* infection (Fig. 4, Tables S7–S10). The flavone and flavonol biosynthesis pathway was significantly enriched in the R accession at 6 hpi but enriched only in the S accession at 24 hpi. Flavonoid metabolism is affected by pathogen infection [27]. Flavone and flavonol biosynthesis and metabolism induce the accumulation of resistant substances to increase antioxidant activity and disease resistance [31]. The R accession initiates a disease response at the early stage [32]; the enrichment of flavone and flavonol biosynthesis and metabolism pathways at this early timepoint may explain its resistance to pathogen infection. Some pathways, including tyrosine metabolism, were significantly enriched, specifically at the late stage of *C. gloeosporioides* infection. Tyrosine is the precursor of several natural compounds, such as phenylalanine and tryptophan [33, 34]. The tyrosine metabolism pathway was significantly enriched among the DEGs in the S accession at 24 hpi, indicating the activation of secondary metabolic synthesis to resist the pathogen.

A greater number of GO terms were enriched in the R accession than in the S accession, especially at 24 hpi. No CC terms were enriched at 6 hpi in either accession, but they were the most enriched in the S accession at 24 hpi, with terms including photosystem II, photosystem II oxygen evolving complex, and oxidoreductase complex. These findings indicate that *C. gloeosporioides* infection disrupted photosynthesis in the leaves of the S accession and that this process was prevented or delayed in the R accession via porphyrin-containing compound biosynthesis [35] and iron ion binding [36]. Moreover, many GO terms were enriched specifically in the S accession. Ubiquitin-protein transferase activity was the GO term enriched specifically in the S accession at 6 and 24 hpi. The ubiquitin proteasome system is the major protein degradation pathway in plants and is related to biotic and abiotic stress tolerance [37–39]. The ubiquitin (Ub) extension protein (UEP) gene NbUEP1 can modulate disease resistance and cell death; RNAi of this gene increases resistance to oomycetes and viruses [40]. *OsPUB41*, an E3 ubiquitin ligase, is induced by PAMPs, and its overexpression in rice increased plant resistance to *Xanthomonas oryzae* pv. *oryzae* [41]. There were fewer significantly enriched GO terms in the S accession than in the R accession; no BP terms were significantly enriched, indicating that the invasion and colonization by pathogenic bacteria were complete. In the S accession, 10 CC terms and 6 MF terms, including those related to the cell wall, apoplast, and thylakoid membrane, were significantly enriched at 24 hpi. In the R accession, only the extracellular region was enriched, suggesting that the *C. gloeosporioides* infection had not entered the cell.

The STEM data revealed that DEG expression changed with time. Profiles with similar trends in R and S accessions were obtained, except for profile 5 of the S accession, whose expression was downregulated at 6 hpi and upregulated at 24 hpi in response to *C. gloeosporioides* infection. The fewest DEGs were observed in profile 5 of accession S (41); these DEGs were significantly enriched in the oxidoreductase activity and dioxygenase activity terms and the flavone and flavonol biosynthesis and tyrosine metabolism pathways. The DEGs included anthocyanidin 3-O-glucosyltransferase 2, flavonoid 3'-monooxygenase, and homogentisate 1,2-dioxygenase. Anthocyanidin-3-O-glucosyltransferases (UFGTs) play key roles in anthocyanin biosynthesis and glycosylation [42]. The expression levels of these genes are related to the levels of anthocyanins [43, 44], which are key substances involved in the abiotic stress response [45, 46]. UFGTs (LITCHI016343.m1) are key genes in the flavone and flavonol biosynthesis pathway. The expression of these genes was downregulated at 6 hpi and then upregulated at 24 hpi in the S accession but downregulated continuously in the R accession. Furthermore, 3 of the 12 UFGT genes were downregulated and then upregulated in the S accession but were not substantially changed or were continuously downregulated in the R accession. This trend towards increased expression may be related to the ability of the pathogen to colonize plant cells. Additionally, in the R accessions, a subset of genes exhibited expression changes only at 6 hpi or 24 hpi, corresponding to profile 3 and profile 4. The genes in profile 3 are predominantly involved in oxidoreductase activity and iron ion binding (Fig. 5, S11). This oxidoreductase activity contributes to defence against pathogens by activating signalling pathways and regulating ion channels and iron reduction, which play crucial roles in plant immune responses [47]. Moreover, genes in C4 are associated with various receptor activities and channel activities. These channel activities are critical for immune responses, as they modulate the flow of calcium ions, triggering downstream calcium-dependent signalling cascades and thus playing a key role in plant immune responses [48]. These channels not only are involved in the rapid response to pathogen aggression but also may regulate internal signalling pathways, which are essential for coordinating long-term defence strategies in plants.

The metabolism of plant hormone signals, such as auxin, gibberellic acid, abscisic acid, ethylene, salicylic acid (SA), and jasmonic acid (JA), is a vital metabolic pathway involved in the response to anthracnose infection [51]. Resistance to biotrophic and hemibiotrophic pathogens relies mainly on the SA-dependent pathway, and the response to necrotrophic pathogens involves JA and ethylene signalling [50–54]. In this study, the expression of eight related genes (one SARU40 gene, two SARU

50 genes, one GH3.1 gene, two DMR6 genes, and one PYL6 gene) changed in response to *C. gloeosporioides* infection. No changes in the expression levels of JA signal-related genes were detected. Thus, it can be inferred that ethylene and auxin are the main hormones involved in resistance to *C. gloeosporioides* in litchi leaves. In addition, multiple pathogenesis-related protein (PR) genes, especially PR1, PR3, PR4B, PRP1, and PTI5, exhibited increased expression with increasing time after *C. gloeosporioides* infection, and the R accession presented a greater advantage. It can be concluded that ethylene signalling, SA signalling, and PR gene expression in litchi induce systemic acquired resistance, resulting in a hypersensitive response in leaves [55]. The resistance reaction in litchi does not involve the JA signal.

WGCNA can be used to classify coexpression modules and select hub genes across all genes. In this study, 2 modules, including 9 hub genes, were identified. The greenyellow module was positively correlated with the R accession at 24 hpi, and its hub genes were related to LRR receptor-like serine/threonine-protein kinase, enoyl-CoA delta isomerase 3, and the E3 ubiquitin-protein ligase RGLG2. Enoyl-CoA delta isomerase participates in linoleic acid metabolism [54] and fatty acid degradation [55]; it is involved in the salt and drought stress response in *Arabidopsis thaliana* [56] and in seed germination [57]. However, there have been no reports on its expression associated with pathogen resistance. The receptor protein PEX5, a peroxisome component, negatively regulates resistance to the blast fungus *Magnaporthe oryzae* in rice. PEX5 is ubiquitinated by APIP6 and degraded via the 26 S proteasome pathway [58]. Our results suggest that enoyl-CoA delta isomerase is located in the peroxisome and that its strong connection with the E3 ubiquitin-protein ligase RGLG2 and the LRR receptor-like serine/threonine-protein kinase suggest that enoyl-CoA delta isomerase 3 may be involved in pathogen resistance. This interaction should be evaluated in further experiments. Notably, the maximum network interaction was observed between the hub genes of the purple and black modules, which also implied associations among kinases, RNA methyltransferases, and ligases.

The primary objective of plant transcriptome sequencing is to elucidate gene expression patterns and regulatory mechanisms comprehensively. In this study, we preliminarily verified that the expression levels of eight genes changed in response to *C. gloeosporioides* infection. The calcium uptake protein, mitochondrial (*MCU*) gene was upregulated exclusively in the R accession. *MCU* is integral to plant disease resistance because it modulates mitochondrial calcium homeostasis and orchestrates downstream signalling pathways that enhance plant defence mechanisms [59]. MCU-mediated calcium influx into mitochondria activates various metabolic pathways, including those involved in energy production and the oxidative burst [60]. The *RPM1* gene has been shown to facilitate a rapid and sustained increase in cytosolic calcium, which is necessary for the oxidative burst and hypersensitive cell death, two key components of plant defence [59].

Transcription factors also play crucial roles in disease resistance. The expression levels of several transcription factor genes were found to be positively correlated with resistance to pathogens (Figs. 7 and 8). Three of these TFs, *WRKY 72*, *ABC1*, *ALDH2*, had their expression verified by using RT-qPCR (Fig. 8), and their patterns of gene expression changes were essentially consistent with the DEG analysis. In the R accessions, the expression levels of these three genes were upregulated at 6 hpi, whereas in the S accessions, expression changes only began at 24 hpi. These results further confirm that resistant accessions initiate immune defences in response to anthracnose infection at an earlier stage [32]. The application of these genes in biotechnological breeding for resistance to anthracnose infection requires further investigation through methods such as genetic transformation and CRISPR.

Conclusion

In this study, 2 litchi accessions were selected from 82 accession resources and subjected to transcriptome analysis to evaluate the molecular mechanisms related to the response to *C. gloeosporioides* infection. The results revealed that the responses involved were related to phenylpropanoid biosynthesis, amino sugar and nucleotide sugar metabolism, plant–pathogen interactions, the MAPK signalling pathway, and the taurine and hypotaurine metabolism pathways. The R accession rapidly initiated a defence in response to *C. gloeosporioides* infection, with increased resistance-related gene expression and flavonoid synthesis, as well as increased antioxidant activity. Moreover, ethylene and SA signalling participated in the resistance reaction. These results provide a foundation for understanding the molecular mechanism of infection resistance in litchi and identifying valuable genes for future studies.

Materials and methods

Plant and fungal materials

For the evaluation of anthracnose disease resistance, 82 litchi natural accession resources (11 years old) of the same age and tree vigour were obtained from the Hainan Province Litchi Accession in Danzhou, China (Supplementary Materials Table S1). This area features a tropical wet and dry climate (Köppen classification: Aw), the annual average temperature is approximately 23.2 °C, and the climatic conditions are conducive to the growth

of litchi. Newly grown branches were obtained, and fresh leaves were selected for inoculation.

Colletotrichum gloeosporioides (09626-4-1-1) was isolated from Huaizhi litchi and was strongly pathogenic when inoculated on leaves.

Inoculation and resistance evaluation

Fresh leaves that had just reached the maximum size (leaf area) were selected and placed in a box with wet tissues. To evaluate resistance, the fresh leaves were inoculated with a mycelial agar disk (5 mm) of *C. gloeosporioides* cultured on potato dextrose agar (PDA). For RNA-seq, leaves were stab-inoculated with a conidial suspension (10^7 conidia/mL) prepared by flooding the surface of the culture plates of *C. gloeosporioides* on synthetic low-nutrient agar (SNA) media with sterile distilled water, filtering the suspension through Miracloth, and adjusting the concentration with sterile distilled water via a haemocytometer.

RNA-seq and data analysis

The leaves were sampled at 0, 6, and 24 h after stab inoculation with a conidial suspension. The samples were discs 1 cm in diameter taken around the inoculation site (including the inoculation site). RNA was collected from 3 biological replicates of inoculated and mock-inoculated plants, and each biological replicate included 20 leaf discs. The samples were immediately frozen in liquid nitrogen and stored at – 80 °C.

Total RNA was extracted via a Plant RNA Kit (Aidlab, Beijing, China), and the RNA concentration and purity were determined via the RNA Nano 6000 Assay Kit for the Bioanalyzer 2100 System (Agilent Technologies, CA, USA). For library preparation, mRNA was purified and used to synthesize cDNA for PCR with Phusion High-Fidelity DNA polymerase, universal PCR primers, and Index (X) Primer. The library preparations were sequenced on an Illumina NovaSeq platform. RNA isolation, RNA quantification and qualification, library preparation, quality inspection, clustering, and sequencing were performed by Novogene (Beijing Novogene Co. Ltd., Beijing, China).

Raw data (raw reads) in fastq format were processed with in-house Perl scripts to obtain clean data. The clean data were mapped to the litchi reference genome (http://www.sapindaceae.com/) via HISAT2 v2.0.5. The database annotation used to determine the functions of the DEGs was performed via Gene Ontology (GO) and Kyoto Encyclopedia of Genes and Genomes (KEGG) enrichment analyses. Short time series expression miner software (STEM) software was used to analyse the DEG expression trends in both the resistant and susceptible accessions [61].

Weighted gene coexpression network analysis (WGCNA)

For the gene coexpression network analysis, a total of 10,416 genes were used as inputs for the signed WGCNA package in TBtools (https://github.com/ShawnWx2019/WGCNA-shinyApp).

A matrix of the normalized expression values of 6000 genes was generated. The FPKM values and phenotypes of the samples were used to identify modules of highly correlated genes. The resulting networks were visualized via Cytoscope software (version 3.10.2) [14].

cDNA synthesis and qRT–PCR analysis

For qPCR and gene expression analysis, first-strand cDNA was synthesized. Then, 1 μg of total RNA was used in the PrimeScript 1st Strand cDNA Synthesis Kit (Thermo Fisher Scientific, Waltham, USA). For gene expression, Real-time reverse transcription PCR analysis was performed via the StepOne™ Real-Time PCR System (Applied Biosystems, Waltham, USA) with TB Green Premix Ex Taq (Takara Bio, Japan) and primers (Table S1). *GAGA-25* was used as the reference gene for expression normalization [62]. The relative gene expression was calculated via the $2^{-\Delta\Delta Ct}$ method.

Supplementary Information

The online version contains supplementary material available at https://doi.org/10.1186/s12870-025-06382-4.

Supplementary Material 1

Supplementary Material 2

Author contributions

J.B.W. conceived and supervised the study; F.L., J.W., L.Z. and Q.Y.L. conducted the experiments; L.Z., X.R.C., H.L.L., S.J.W., G.W., and X.X.L. assisted with the experiments; F.L., J.W., and J.B. W. analyzed the data; F.L. and J.B.W. wrote the manuscript. All authors read and approved the manuscript.

Funding

This research was funded by Science and Technology Special Fund of Hainan Province (Grant No. ZDYF2021XDNY159 and ZDYF2021XDNY156); Central Public-interest Scientific Institution Basal Research Fund (Grant No. 1630032022007); China Agricultural Research System of MOF and MARA (Grant No. CARS-32-01).

Data availability

Sequence data that support the findings of this study have been deposited in the National Center for Biotechnology Information with the accession number PRJNA1157370.

Declarations

Ethics approval and consent to participate

The experiments were carried out with the permission of relevant agencies. Leaves were obtained from Danzhou, Hainan, China. All of the experiments were carried out in accordance with relevant guidelines and regulations.

Consent for publication

Not applicable.

Competing interests

The authors declare no competing interests.

Received: 29 September 2024 / Accepted: 11 March 2025
Published online: 26 March 2025

References

1. Sudheeran PK, Sela N, Carmeli-Weissberg M, Ovadia R, Panda S, Feygenberg O, Maurer D, Oren-Shamir M, Aharoni A, Alkan N. Induced defense response in red Mango fruit against *Colletotrichum gloeosporioides*. Hortic Res. 2021;8(1):17.
2. Wang W, de Silva DD, Moslemi A, Edwards J, Ades PK, Crous PW, Taylor PWJ. Colletotrichum species causing anthracnose of citrus in Australia. J Fungi. 2021;12(7):1–47.
3. Castellar C, Petermann D, May De Mio LL. Epidemiological relevance of *Colletotrichum* species isolated from glomerella leaf spot causing symptoms in Apple fruit. Plant Dis. 2023;107(11):3403–13.
4. Tan Q, Schnabel G, Chaisiri C, Yin L, Yin W, Luo C. *Colletotrichum* species associated with peaches in China. J Fungi (Basel). 2022;8(3):313.
5. Hu G, Feng J, Xiang X, Wang J, Salojärvi J, Liu C, Wu Z, Zhang J, Liang X, Jiang Z, Liu W, Ou L, Li J, Fan G, Mai Y, Chen C, Zhang X, Zheng J, Zhang Y, Peng H, Yao L, Wai CM, Luo X, Fu J, Tang H, Lan T, Lai B, Sun J, Wei Y, Li H, Chen J, Huang X, Yan Q, Liu X, McHale LK, Rolling W, Guyot R, Sankoff D, Zheng C, Albert V, Ming R, Chen H, Xia R, Li J. Two divergent haplotypes from a highly heterozygous lychee genome suggest independent domestication events for early and late-maturing cultivars. Nat Genet. 2022;54(1):73–83.
6. Zhao J, Yu Z, Wang Y, Li Q, Tang L, Guo T, Huang S, Mo J, Hsiang T. Litchi anthracnose caused by Colletotrichum karstii in Guangxi, China. Plant Dis. 2021;21.
7. Cao X, Li F, Xu H, Li H, Wang S, Wang G, West JS, Wang J. Characterization of *Colletotrichum* species infecting Litchi in Hainan, China. J Fungi (Basel). 2023;9(11):1042.
8. Huang R, Sun W, Guo T, Huang S, Tang L, Chen X, Li Q. Morphological and pathological characterization of *Colletotrichum* species causing anthracnose of Litchi leaves in Guangxi, China. J Phytopathol. 2023;171:609.
9. Wang S, Zeng X, Wang X, Chang H, Sun H, Liu Y. A survey of multiple pesticide residues on Litchi: A special fruit. Microchem J. 2022;175:107175.
10. Wu S, Zhen C, Wang K, Gao H. Effects of *Bacillus subtilis* CF-3 VOCs combined with heat treatment on the control of *Monilinia fructicola* in peaches and *Colletotrichum gloeosporioides* in Litchi fruit. J Food Sci. 2019;84(12):3418–28.
11. Yuan M, Jiang Z, Bi G, Nomura K, Liu M, Wang Y, Cai B, Zhou J, He S, Xin X. Pattern-recognition receptors are required for NLR-mediated plant immunity. Nature. 2021;592(7852):105–9.
12. Barakat A, Staton M, Cheng C, Park J, Yassin N, Ficklin S, Yeh C, Hebard F, Baier K, Powell W, Schuster S, Wheeler N, Abbott A, Carlson J, Sederoff R. Chestnut resistance to the blight disease: insights from transcriptome analysis. BMC Plant Biol. 2012;12:38.
13. Dorostkar S, Dadkhodaie A, Ebrahimie E, Heidari B, Ahmadi-Kordshooli M. Comparative transcriptome analysis of two contrasting resistant and susceptible *Aegilops Tauschii* accessions to wheat leaf rust (*Puccinia triticina*) using RNA-sequencing. Sci Rep. 2022;12(1):821.
14. Shannon P, Markiel A, Ozier O, Baliga N, Wang J, Ramage D, Amin N, Schwikowski B, Ideker T. Cytoscape: a software environment for integrated models of biomolecular interaction networks. Genome Res. 2003;13(11):2498–504.
15. Dowling M, Peres N, Villani S, Schnabel G. Managing *Colletotrichum* on fruit crops: A complex challenge. Plant Dis. 2020;104(9):2301–16.
16. Jiang L, Zhang S, Su J, Peck SC, Luo L. Protein kinase signaling pathways in plant-*Colletotrichum* interaction. Front Plant Sci. 2022;12:829645.
17. Hu L, Yang L. Time to fight: molecular mechanisms of age-related resistance. Phytopathology. 2019;109(9):1500–8.
18. Singh B, Delgado-Baquerizo M, Egidi E, Guirado E, Leach J, Liu H, Trivedi P. Climate change impacts on plant pathogens, food security and paths forward. Nat Rev Microbiol. 2023;21(10):640–56.
19. Shirima R, Legg J, Maeda D, Tumwegamire S, Mkamilo G, Mtunda K, Kulembeka H, Ndyetabula I, Kimata B, Matondo D, Ceasar G, Mushi E, Sichalwe K, Kanju E. Genotype by environment cultivar evaluation for cassava brown streak disease resistance in Tanzania. Virus Res. 2020;286:198017.
20. Hua J. Modulation of plant immunity by light, circadian rhythm, and temperature. Curr Opin Plant Biol. 2013;16(4):406–13.
21. Verhaegen M, Bergot T, Liebana E, Stancanelli G, Streissl F, Mingeot-Leclercq M, Mahillon J, Bragard C. On the use of antibiotics to control plant pathogenic bacteria: a genetic and genomic perspective. Front Microbiol. 2023;14:1221478.
22. Blundell R, Schmidt J, Igwe A, Cheung A, Vannette R, Gaudin A, Casteel C. Organic management promotes natural pest control through altered plant resistance to insects. Nat Plants. 2020;6(5):483–91.
23. Wang Y, Hao X, Lu Q, Wang L, Qian W, Li N, Ding C, Wang X, Yang Y. Transcriptional analysis and histochemistry reveal that hypersensitive cell death and H_2O_2 have crucial roles in the resistance of tea plant (*Camellia sinensis* (L.) O. Kuntze) to anthracnose. Hortic Res. 2018;5:18.
24. Yang M, Zhou C, Yang H, Kuang R, Liu K, Huang B, Wei Y. Comparative transcriptomics and genomic analyses reveal differential gene expression related to *Colletotrichum brevisporum* resistance in Papaya (*Carica Papaya* L). Front Plant Sci. 2022;13:1038598.
25. Guan F, Shi B, Zhang J, Wan X. Transcriptome analysis provides insights into lignin synthesis and MAPK signaling pathway that strengthen the resistance of bitter gourd (*Momordica charantia*) to fusarium wilt. Genomics. 2023;115(1):110538.
26. Tang B, Feng L, Hulin MT, Ding P, Ma W. Cell-type-specific responses to fungal infection in plants revealed by single-cell transcriptomics. Cell Host Microbe. 2023;31(10):1732–e17475.
27. Hazra A, Ghosh S, Naskar S, Rahaman P, Roy C, Kundu A, Chaudhuri R, Chakraborti D. Global transcriptome analysis reveals fungal disease responsive core gene regulatory landscape in tea. Sci Rep. 2023;13(1):17186.
28. Alvarez-Diaz JC, Laugé R, Delannoy E, Huguet S, Paysant-Le Roux C, Gratias A, Geffroy V. Genome-wide transcriptomic analysis of the effects of infection with the hemibiotrophic fungus *Colletotrichum lindemuthianum* on common bean. Plants. 2022;11(15):1995.
29. Kanwar P, Jha G. Alterations in plant sugar metabolism: signatory of pathogen attack. Planta. 2019;249(2):305–18.
30. Lee D, Ahn S, Cho H, Yun H, Park J, Lim J, Lee J, Kwon S. Metabolic response induced by parasitic plant-fungus interactions hinder amino sugar and nucleotide sugar metabolism in the host. Sci Rep. 2016;6:37434.
31. Nabavi S, Šamec D, Tomczyk M, Milella L, Russo D, Habtemariam S, Suntar I, Rastrelli L, Daglia M, Xiao J, Giampieri F, Battino M, Sobarzo-Sanchez E, Nabavi S, Yousefi B, Jeandet P, Xu S, Shirooie S. Flavonoid biosynthetic pathways in plants: versatile targets for metabolic engineering. Biotechnol Adv. 2020;38:107316.
32. Nida H, Lee S, Li Y, Mengiste T. Transcriptome analysis of early stages of sorghum grain mold disease reveals defense regulators and metabolic pathways associated with resistance. BMC Genom. 2021;22(1):295.
33. Maeda H, Dudareva N. The Shikimate pathway and aromatic amino acid biosynthesis in plants. Annu Rev Plant Biol. 2012;63:73–105.
34. Yao L, Li Y, Ma C, Tong L, Du F, Xu M. Combined genome-wide association study and transcriptome analysis reveal candidate genes for resistance to *Fusarium* ear rot in maize. J Integr Plant Biol. 2020;62(10):1535–51.
35. Das R, Kumar Verma P, Nagaraja C. Design of porphyrin-based frameworks for artificial photosynthesis and environmental remediation: recent progress and future prospects. Coord Chem Rev. 2024;514:215944.
36. Haschka D, Hoffmann A, Weiss G. Iron in immune cell function and host defense. Semin Cell Dev Biol. 2021;115:27–36.
37. Xu F, Xue H. The ubiquitin-proteasome system in plant responses to environments. Plant Cell Environ. 2019;42(10):2931–44.
38. Xu J, Liu H, Zhou C, Wang J, Wang J, Han Y, Zheng N, Zhang M, Li X. The ubiquitin-proteasome system in the plant response to abiotic stress: potential role in crop resilience improvement. Plant Sci. 2024;342:112035.
39. Méndez-Gómez M, Sierra-Cacho D, Jiménez-Morales E, Guzmán P. Modulation of early gene expression responses to water deprivation stress by the E3 ubiquitin ligase ATL80: implications for retrograde signaling interplay. BMC Plant Biol. 2024;24(1):180.
40. Xu Y, Zhao Y, Song X, Ye Y, Wang R, Wang Z, Ren X, Cai X. Ubiquitin extension protein UEP1 modulates cell death and resistance to various pathogens in tobacco. Phytopathology. 2019;109(7):1257–69.
41. Kachewar N, Gupta V, Ranjan A, Patel H, Sonti R. Overexpression of OsPUB41, a rice E3 ubiquitin ligase induced by cell wall degrading enzymes, enhances immune responses in rice and Arabidopsis. BMC Plant Biol. 2019;19(1):530.
42. Wang H, Wang C, Fan W, Yang J, Appelhagen I, Wu Y, Zhang P. A novel glycosyltransferase catalyses the transfer of glucose to glucosylated anthocyanins in purple sweet potato. J Exp Bot. 2018;69(22):5444–59.
43. Li X, Li Y, Zhao M, Hu Y, Meng F, Song X, Tigabu M, Chiang VL, Sederoff R, Ma W, Zhao X. Molecular and metabolic insights into anthocyanin biosynthesis for leaf color change in chokecherry (*Padus virginiana*). Int J Mol Sci. 2021;22(19):10697.

44. Filyushin M, Shchennikova A, Kochieva Z. Antocyandin-3-*O*-Glucosyltransferase genes in pepper (*Capsicum* spp.) and their role in anthocyanin biosynthesis. Russ J Genet. 2023;59:441–52.
45. Landi M, Tattini M, Gould K. Multiple functional roles of anthocyanins in plant-environment interactions. Environ Exp Bot. 2015;119:4–17.
46. Kaur S, Tiwari V, Kumari A, Chaudhary E, Sharma A, Ali U, Garg M. Protective and defensive role of anthocyanins under plant abiotic and biotic stresses: an emerging application in sustainable agriculture. J Biotechnol. 2023;361:12–29.
47. Yan J, Feng Z, Xiao Y, Zhou M, Zhao X, Lin X, Shi W, Busch W, Li B. ANAC044 orchestrates mitochondrial stress signaling to trigger iron-induced stem cell death in root meristems. Proc Natl Acad Sci U S A. 2025;7(1):e2411579122.
48. Tian W, Hou C, Ren Z, Wang C, Zhao F, Dahlbeck D, Hu S, Zhang L, Niu Q, Li L, Staskawicz BJ, Luan S. A calmodulin-gated calcium channel links pathogen patterns to plant immunity. Nature. 2019;572(7767):131–5.
49. Bari R, Jones JD. Role of plant hormones in plant defence responses. Plant Mol Biol. 2009;69:473–88.
50. Glazebrook J. Contrasting mechanisms of defense against biotrophic and necrotrophic pathogens. Annu Rev Phytopathol. 2005;43:205–27.
51. Tsuda K, Mine A, Bethke G, Igarashi D, Botanga C, Tsuda Y, Glazebrook J, Sato M, Katagiri F. Dual regulation of gene expression mediated by extended MAPK activation and Salicylic acid contributes to robust innate immunity in *Arabidopsis Thaliana*. PLoS Genet. 2013;9(12):e1004015.
52. Shi Y, Sheng Y, Cai Z, Yang R, Li Q, Li X, Li D, Guo X, Lu J, Ye J, Wang K, Zhang L, Liang Y, Zheng X. Involvement of Salicylic acid in anthracnose infection in tea plants revealed by transcriptome profiling. Int J Mol Sci. 2019;20(10):2439.
53. Noman A, Aqeel M, Qari SH, Al Surhanee A, Yasin G, Alamri S, Hashem M, Al-Saadi M. Plant hypersensitive response vs pathogen ingression: death of few gives life to others. Microb Pathog. 2020;145:104224.
54. Gerhardt B, Kleiter A. Peroxisomal catabolism of Linoleic acid. In: Kader JC, Mazliak P, editors. Plant lipid metabolism. Springer Dordrecht; 1995.
55. Allenbach L, Poirier Y. Analysis of the alternative pathways for the beta-oxidation of unsaturated fatty acids using Transgenic plants synthesizing polyhydroxyalkanoates in peroxisomes. Plant Physiol. 2000;124(3):1159–68.
56. Peng R, Xu Y, Tian S, Unver T, Liu Z, Zhou Z, Cai X, Wang K, Wei Y, Liu Y, Wang H, Hu G, Zhang Z, Grover C, Hou Y, Wang Y, Li P, Wang T, Lu Q, Wang Y, Conover J, Ghazal H, Wang Q, Zhang B, Van Montagu M, Van de Peer Y, Wendel J, Liu F. Evolutionary divergence of duplicated genomes in newly described allotetraploid cottons. Proc Natl Acad Sci U S A. 2022;119(39):e2208496119.
57. Goepfert S, Vidoudez C, Rezzonico E, Hiltunen J, Poirier Y. Molecular identification and characterization of the Arabidopsis delta(3,5), delta(2,4)-dienoyl-coenzyme A isomerase, a peroxisomal enzyme participating in the beta-oxidation cycle of unsaturated fatty acids. Plant Physiol. 2005;138(4):1947–56.
58. You X, Zhu S, Sheng H, Liu Z, Wang D, Wang M, Xu X, He F, Fang H, Zhang F, Wang D, Hao Z, Wang R, Xiao Y, Wan J, Wang G, Ning Y. The rice peroxisomal receptor PEX5 negatively regulates resistance to rice blast fungus *Magnaporthe oryzae*. Cell Rep. 2023;42(10):113315.
59. Yamada A, Watanabe A, Yamamoto T. Regulatory mechanisms of mitochondrial calcium uptake by the calcium uniporter complex. Biophys Physicobiol. 2023;20(1):e200004.
60. Wang C, Tang R, Kou S, Xu X, Lu Y, Rauscher K, Voelker A, Luan S. Mechanisms of calcium homeostasis orchestrate plant growth and immunity. Nature. 2024;627:382–8.
61. Ernst J, Bar-Joseph Z. STEM: a tool for the analysis of short time series gene expression data. BMC Bioinformatics. 2006;7:191.
62. Li F, Sun J, Men J, Li H, Wang G, Wang S, Wang J. Selection and validation of reference genes for RT-qPCR analysis in the pericarp of *Litchi chinensis*. Biol Plant. 2022;66:103–11.

Publisher's note